Automated Measurement of Fracture Callus in Radiographs Using Portable Software

Stephen M. Porter,[1] Hannah L. Dailey,[2] Katherine A. Hollar,[3] Karina Klein,[4] James A. Harty,[5] Trevor J. Lujan[3]

[1]Department of Computer Science, Boise State University, 1910 University Drive, Boise, Idaho 83725-2055, [2]Department of Mechanical Engineering and Mechanics, Lehigh University, 19 Memorial Dr W, Bethlehem, Pennsylvania 18015, [3]Department of Mechanical and Biomedical Engineering, Boise State University, 1910 University Drive, Boise, Idaho 83725-2085, [4]Competence Center for Applied Biotechnology and Molecular Medicine, Equine Hospital, Vetsuisse Faculty, University of Zurich, Winterthurerstrasses 260, CH-8057, Zurich, Switzerland, [5]Cork University Hospital, University College Cork, Wilton, Cork, Ireland

ABSTRACT: The development of software applications that assist the radiographic evaluation of fracture healing could advance clinical diagnosis and expedite the identification of effective treatment strategies. A radiographic feature regularly used as an outcome measure for basic and clinical fracture healing research is new bone growth, or fracture callus. In this study, we developed OrthoRead, a portable software application that uses image-processing algorithms to detect and measure fracture callus in plain radiographs. OrthoRead utilizes an optimal boundary tracking algorithm to semi-automatically segment the cortical surface, and a novel iterative thresholding selection algorithm to then automatically segment the fracture callus. The software was validated in three steps. First, algorithm accuracy and sensitivity were analyzed using surrogate models with known callus size. Second, the callus area of distal femur fractures measured using OrthoRead was compared to callus area manually outlined by orthopaedic surgeons. Third, the callus area of ovine tibial fractures was measured using OrthoRead and compared to callus volume measured from micro-CT. The software had less than a 5% error in measuring surrogate callus, and was insensitive to changes in image resolution, image rotation, and the size of the analyzed region of interest. Strong positive correlations existed between OrthoRead and clinicians ($R^2 = 0.98$), and between 2D callus area and 3D callus volume ($R^2 = 0.70$). The average run time for OrthoRead was 3 s when using a 2.7 GHz processor. By being accurate, fast, and robust, OrthoRead can support prospective and retrospective clinical studies investigating implant efficacy, and can assist research on fracture healing mechanobiology. © 2015 Orthopaedic Research Society. Published by Wiley Periodicals, Inc. J Orthop Res 34:1224–1233, 2016.

Keywords: segmentation; fracture; callus; radiography; computer aided diagnosis

Delayed union and non-union of fractured bones continue to be a persistent problem in orthopaedic medicine. Notably, reoperation rates in surgically treated fractures of the tibia have been reported at 14–27%,[1] while reoperation rates for distal femur fractures have been reported between 13% and 21%.[2,3] Poor healing outcomes come at a high fiscal cost to hospitals, patients, and workplaces.[4] A clear medical challenge is to identify the most effective treatment interventions for specific indications. A barrier to addressing this challenge is the absence of universally recognized guidelines to evaluate fracture union from plain radiographs or X-rays. While the acquisition and evaluation of X-rays during post-operative clinical visits is a standard in fracture care,[5] there is no standard for radiographic assessment.[6–9] The absence of standard assessment techniques is reflected by the 20–25% inter-observer variability reported by clinicians analyzing radiographs for fracture healing.[10,11] The development of computer vision technology to automate the detection of important radiographic features could improve the objectivity of radiographic assessment and therefore, provide reliable outcome measures to evaluate treatment strategies.

An anatomical feature on radiographs that has clinical relevance to fracture healing is new bone growth, or fracture callus (Fig. 1). Fracture callus is a heterogeneous tissue composed of hyaline cartilage, fibrous tissue, and woven bone that forms near the fracture site. Callus will eventually bridge the fracture gap and remodel into strong lamellar bone. The size of callus formation in radiographs is predictive of bending stiffness, and thus relates to mechanical stability at the fracture site.[12,13] Therefore, the presence of callus in radiographs is regularly used as an outcome measure in basic and clinical research.[9] Recently, callus formation has been incorporated into standardized scoring systems to assess healing in fractures of the tibia and pelvis.[14,15] However, a software standard for detecting fracture callus in plain radiographs has not yet been established, and most methods of measuring callus are qualitative in nature.[14,15]

Many challenges exist in the development of an automated tool to quantify fracture callus. These challenges include the morphological diversity of bone fractures, radiographic noise, and the heterogeneous soft-tissue envelope that obscures the clarity of the cortex and the fracture callus (Fig. 1). Additionally, the pixel intensity of callus is highly variable as the callus matures over time from cartilaginous tissue to mineralized lamellar bone. To overcome these challenges, callus size has been estimated using a "Callus Index," or the ratio of maximum callus diameter relative to bone diameter,[13] and by using image processing software for semi-automated segmentation.[16,17] However, the objectivity, efficiency, and accuracy of these methods have
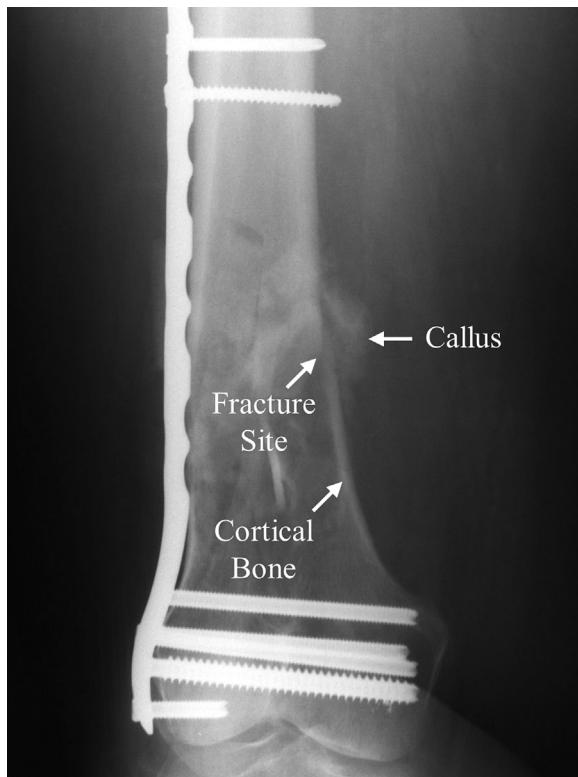
Figure 1. Plain radiograph of a distal femur fracture treated with a locked plating construct at 12 weeks post-surgery. The discontinuity in the cortical bone at the fracture site is bridged by fracture callus.

not been reported. More recently, a custom Matlab program (Mathworks, Natwick MA) was developed to automate the measurement of callus area.[18] While this Matlab program successfully supported clinical retrospective studies of fracture fixation devices,[19,20] the program had severe limitations that precluded a widespread adoption by clinicians and scientists. These limitations included the proprietary Matlab software environment, absence of a graphic user interface, slow processing time, and segmentation algorithms that were sensitive to large image rotations and were based on fixed thresholding methods that inhibited robust operation.

In order to make automated callus detection a practical research and clinical tool for public use, the segmentation algorithms must be robust and independent of operator action. Further, these segmentation algorithms must be rigorously validated and implemented into a software application that is portable to a user's preferred operating system. The objective of this research is to develop and validate robust algorithms to automate the accurate segmentation of fracture callus in plain radiographs, and to implement these algorithms into a portable software that is free to the public.

MATERIALS AND METHODS
Image processing algorithms that measure fracture callus in digital plain radiographs were incorporated into OrthoRead,

a portable Java application that is free to download (Fig. 2A; http://coen.boisestate.edu/ntm/orthoread/). OrthoRead requires users to crop a region of interest (ROI, Fig. 2B), and then select seed points on the cortex surface (Fig. 2C). The periosteal cortex surface and the fracture callus surface are then automatically segmented using a boundary tracking algorithm and novel iterative threshold selection (ITS) algorithm, respectively (Fig. 2D). Callus size is converted to metric area and displayed.

Cortex Segmentation
Cortex segmentation uses an optimal boundary tracking method, known as intelligent scissors.[21] This algorithm requires the user to define at least two seed points on the external cortex of each fracture fragment. The user is instructed to select the first seed point near the fracture site and the last seed point near the ROI boundary (Fig. 2C). To ensure that all cortical surfaces are segmented within the ROI, the algorithm automatically defines seed points on the ROI boundary. The coordinates of this boundary seed point are defined by interpolating the two seed points nearest the ROI boundary to calculate a slope-intercept equation, and then extrapolating a straight line until the ROI boundary is reached.

All seed point positions are input into the optimal boundary tracking method, and a series of local cost functions detect the external cortex boundary.[21] The independent cortical fragments are then connected by the shortest line between the tip of the most distal cortex with the periosteal surface of the proximal cortex.[18] Once the cortex is defined, the image is classified into two distinct regions: Endosteal and periosteal. The endosteal region is located inside the cortical bone surface, while the periosteal region is located outside the cortical bone surface and contains the fracture callus. The endosteal and periosteal

Figure 2. Callus detection using OrthoRead software. (A) The graphic user interface has navigation tools to help select a (B) Region of Interest (ROI) around the fracture site. (C) In the ROI, the user selects two or more seed point points on the surface of the bone fragments (white cross, top fragment seed point; black cross, bottom fragment seed point). (D) The periosteal cortex surface (black line) and callus surface (white line) are then automatically segmented.

regions are automatically classified by calculating the average local pixel value on either side of the cortex, where the side with the highest average pixel value is assigned as the endosteal region.

Callus Segmentation

After cortex segmentation, periosteal callus is automatically detected in the ROI using an ITS algorithm. This algorithm identifies an optimal gradient threshold by analyzing a series of potential solutions. In the first part of the ITS method, an image stack is built by applying sequential threshold values to a single gradient image of the digital radiograph. The two-dimensional spatial gradient image is generated using a Sobel operator in the periosteal region. A stack of binary images is then produced at each threshold level, where pixels exceeding the specified threshold are given a value of 255 and all other pixels are given a value of zero. For each binary image, morphological dilation and flood fill watershed operations are applied to create blobs. Any blob not connected to the segmented cortex is eliminated and remaining blobs are considered callus. The callus surface is smoothed using morphological opening and closing operations.

The second part of the ITS algorithm is to identify the best threshold level based on data extracted from the image stack. This optimization process uses normalized parameters collected at each threshold: Callus contraction terms, β and β', and an outward gradient term, κ.

Callus Contraction

The scalar variable β is the percent reduction in callus size, c, at each threshold level, t:

$$\beta(t) = \frac{c_t - c_{t-1}}{c_{t-1}} * 100 \tag{1}$$

The rolling average of callus contraction, β', is also calculated:

$$\beta'(t) = \frac{\beta_{t-1} + \beta_t + \beta_{t+1}}{3} \tag{2}$$

Outward Gradient

The variable κ is the percentage of pixels on the callus surface that have a negative gradient vector relative to the proximal periosteal pixels. This is described using the scalar function:

$$\kappa = \sum_{v \in S} \left(g(v)/n \right) \left(*100 \right) \tag{3}$$

where S is the set of all n position vectors, v, on the outer edge of the callus. The function $g(v)$ is determined with the conditional statement:

$$g(v) = \begin{cases} 1 & if \dfrac{\partial p(v)}{\partial x} \cdot n(v) < 0 \\ 0 & if \dfrac{\partial p(v)}{\partial x} \cdot n(v) \geq 0 \end{cases} \tag{4}$$

where, p is the pixel intensity at v, and n is a unit normal vector at position v pointing outward from the callus edge. The scalar product of n and the gradient of p is taken for all position vectors v in the set S. Numerically, this algorithm was implemented by traversing the callus edge and performing a 4-neighbor check on each callus edge pixel to calculate the average intensity difference between the callus edge pixel and background pixel(s). If no neighbor pixels were detected in the background, an 8-neighbor check was used and the average difference was calculated between the callus edge pixel and background pixels. Visually, a callus object with a high κ value has a distinct edge with greater intensity than the background region.

Threshold Optimization

The callus contraction terms, β and β', are used to identify the lower bound and upper bound for the optimized threshold value. The lower threshold bound is picked when β decreases below 10% to a local minimum, while the subsequent upper bound is picked when β' reaches a local minimum below 10%. The optimized threshold value is the first local κ maximum ($\pm 1\%$) that occurs between the lower and upper threshold bound (Fig. 3A). The optimized threshold will occur when the callus area stabilizes (Fig. 3B–D). OrthoRead will display segmentation results using this optimized threshold (Fig. 3D). Other local κ maximums may occur between the upper and lower bound (Fig. 3E), but empirical evidence suggests that the first local maximum gives the best
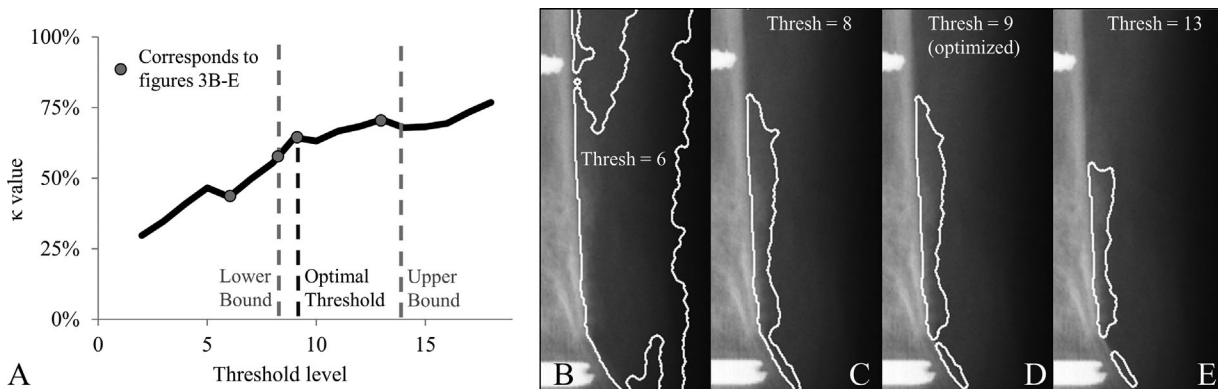
Figure 3. Optimization of threshold selection. (A) Normalized parameters (κ, β, β') are calculated for a sequence of threshold values, and lower and upper bounds are identified using local minima of β and β'. (B) At low threshold levels, callus area is overestimated. (C and D) Callus area then stabilizes between threshold levels, and (D) an optimal threshold is selected as the first local κ maxima inside the bounds. This maxima is more accurate than (E) secondary local maxima that could underestimate callus size.

approximation of callus. If a local maximum does not occur between the upper and lower bound, then the optimized threshold value is selected at the upper bound. An additional criterion for the optimized threshold value is that κ must exceed 50%. An important aspect of these threshold optimization criteria is that they act independently of ROI size and image resolution and therefore, are less sensitive to user operations. The computational cost of this optimization process was reduced by implementing recursive operations and by using a look-ahead algorithm to select the upper bound and thus limit the size of the image stack.

Cortical Bridging

The fracture site was determined bridged if the segmented cortices and callus created a continuous connection between the ROI boundaries.[22] This was numerically implemented by checking whether the two cortical fragments intersected at any point or if the cortical fragments were both contiguous to the same callus object.

Unit Conversion

Conversion to metric area was achieved using a known dimension of an image feature. This can be performed manually, where the user draws a line between two points of known metric length, and the corresponding number of line pixels is then used to calculate a pixel-to-metric conversion factor. Alternatively, the program can automatically draw this line by using a Sobel edge detection filter to automatically generate a line between feature edges. This auto feature is practical for radiographic images that display a side-view of cylindrical hardware (e.g., screws, nails). If known, the user can also enter the image's pixels per inch (PPI).

Accuracy and Sensitivity

The effect of user-defined actions on algorithm accuracy was quantified using a callus surrogate model. A three-dimensional surrogate model of a callus was previously manufactured with known dimensions ($274\,mm^2$).[18] Briefly, the surrogate was assembled by press-fitting cortical components (Sawbones, Vashon WA) into a callus that was composed of epoxy and fiberglass. After radiographs of the surrogate were captured (70 kV, 0.06 s) and digitized, a soft tissue envelope was superimposed upon the image and a volume preserving

transformation was applied to give curvature (Fig. 4). The effect of image resolution and PPI on algorithm accuracy was tested by measuring surrogate callus at incremental image rotations of 45°, and at image resolutions of 100, 200, and 300 PPI. Although rotations between 0 and 45° will cause small variations in distortion due to the rotation transformation operation, the rationale for examining the effect of large image rotations in increments of 45° is that prior algorithms for segmenting callus were highly sensitive to large rotations and required the long axis of the bone to be nearly vertical.[18] Therefore, we wanted to determine if our algorithm was invariant to large rotations. In addition, the effect of cortex seed point location on algorithm accuracy was tested by translating the seed points by up to 5 mm (twice the cortical thickness) normal or tangential to a frame of reference on the cortical surface. Normal translation was performed distal and proximal to the frame of reference, while tangential translation was performed superior and inferior to the frame of reference.

The sensitivity of the algorithm to changes in ROI size was tested by measuring callus in clinical radiographs while increasing the ROI by up to 400%. To compare the performance of the ITS method to established methods, this analysis was also performed after replacing the ITS algorithm with two standard algorithms for optimizing a global threshold: The Otsu and IsoData methods.[23,24] All methods were applied to the gradient image of the radiograph. For this comparison, the detected callus size at each ROI level was normalized to the average callus size at all ROI levels.

Clinical Validation

Clinical validation of the ITS algorithm was determined by quantifying callus in ten anteroposterior and lateral radiographs of distal femur fractures at a post-operative time point. Results from this analysis were compared with published results of the callus area in these same radiographs when measured by three orthopaedic surgeons.[18] In brief, clinicians used a pen tablet to manually outline the cortex and periosteal callus in each digital radiograph, and callus area was computed from the digitally marked outlines. Three undergraduate engineering students independently evaluated the same ten clinical radiographs using OrthoRead (image resolution = 180 ± 13 PPI), and callus size was measured for comparison to the clinicians' results.
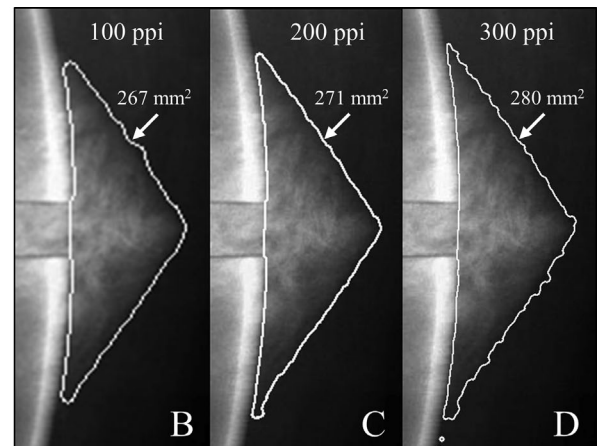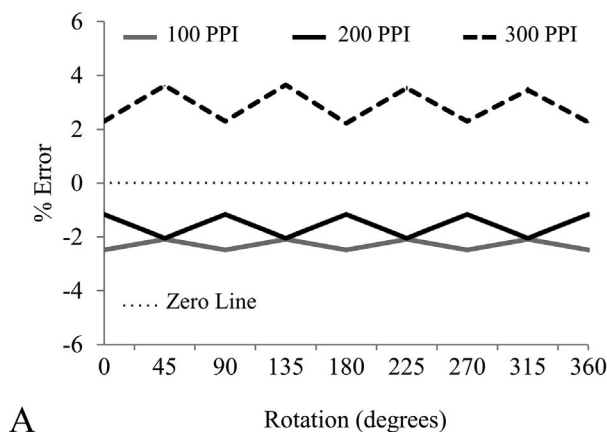
Figure 4. Effect of image resolution and image rotation on accuracy. (A) Error was affected by 45° increments in rotation. (B–D) More callus was measured in images with greater PPI.

Experimental Validation

The experimental validity of using two-dimensional (2D) callus area to represent the three-dimensional (3D) callus morphology was determined by analyzing images from plain radiography and microcomputed tomography (μCT) of skeletally mature female sheep (sample size = 18, age 2.5–3 years). All animals received transverse midshaft tibial osteotomies and fracture fixation by reamed intramedullary (IM) nailing. After 9 weeks, the sheep were euthanized and anteroposterior (AP) and mediolateral (ML) plain radiographs were recorded of the excised tibias (image resolution = 110 ± 2 PPI). The same excised tibias were also imaged using quantitative μCT scanning with a nominal isotropic resolution of 49.2 μm. OrthoRead was used on both the AP and ML radiographic plain films to segment four cortices—anterior, posterior, medial, and lateral—and provided projected area measures for each view of the periosteal callus. Pixel area was converted to dimensional area by identifying a reference geometry of known size, the IM nail proximal stem. Segmentation and 3D reconstruction of the μCT scans was performed using a commercially available software package (Analyze 12.0; Analyze Direct, Overland Park, KS). Using Analyze, periosteal callus in the μCT images was distinguished from cortical bone with a combination of intensity thresholding and spline-based region detection. Individual global thresholds were used to segment dense cortical bone[25] and a fixed global threshold was used to segment callus from the soft-tissue envelope.[26] The spline operation ensured that the sagittal external cortex maintained linearity from the distal shaft to the midshaft osteotomy. The software then automatically converted the segmented image stack into 3D reconstructions of the periosteal callus and cortical bone. The volume of the periosteal callus from the μCT was then compared to the sum of the four periosteal area projections from the plain radiographs. All animal experiments were conducted according to Swiss laws of animal protection and welfare and were authorized by the cantonal ethical committee.

Statistical Analysis

The effect of image rotation, image resolution, ROI size, and location of cortex seed points on callus area was assessed using a univariate analysis of variance. Tukey post-hoc tests determined significance between factor levels. Accuracy in measuring the callus area of the surrogate model was defined by the mean percentage error, $(area_{measured} - area_{actual})/area_{actual}$. Differences in callus area between the algorithm and clinicians, and between callus area using the algorithm and callus volume using μCT, were tested with a Pearson r correlation.

RESULTS

OrthoRead measured periosteal fracture callus for all images without a programming error. When analyzing clinical radiographs, the average total runtime for segmenting both the cortex and callus was 3.0 ± 0.2 s.

Sensitivity to Image Rotation and Resolution

The average error when measuring surrogate callus size at variable image resolutions and rotations was 0.3 ± 2.3% (Fig. 4A). The lowest error occurred at image resolutions of 200 PPI. Rotating the image by 90° increments had no effect on error, but rotating the image by 45° increments did affect error ($p < 0.01$). As PPI increased, the size of the measured callus also increased (Fig. 4B–D, $p < 0.01$).

Sensitivity to Cortex Segmentation

The average error when measuring surrogate callus size at variable seed point positions was 1.3 ± 1% (Fig. 5A). When seed points were located directly on each cortex, the error was 1.2 ± 0.1% (Fig. 5B). Error increased significantly when a seed point was moved normal to the cortex at the fracture site ($p < 0.01$), with a maximum error of 5.5% (Fig. 5C). There was no change in error when seed points were moved normal to the cortex at the ROI border (Fig. 5D), or when seed points were moved tangential to the cortex (Fig. 5A).

Sensitivity to ROI Area

The measurement of callus size in ten clinical radiographs was not affected by ROI area when using the proposed ITS algorithm (Fig. 6A). However, the
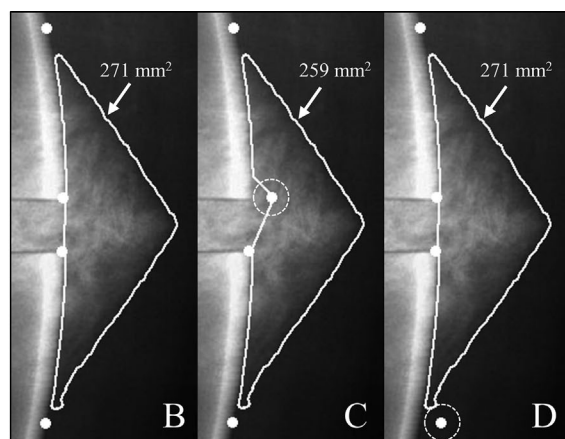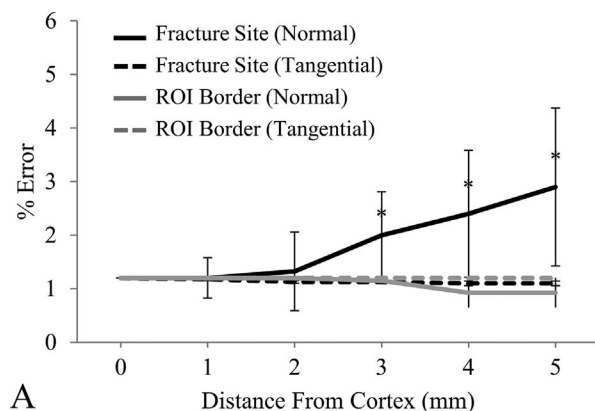
Figure 5. Effect of cortex seed point position on error when measuring surrogate callus. (A) Error as a function of seed point distance from cortex surface. (B) Seed point positions were selected directly on cortex surface as a frame of reference (white dots, distance from cortex = 0 mm). (C) Error increased when seed points were shifted normal to the cortex near the fracture site (dashed circle, distance from cortex = 5 mm), (D) but error did not increase when seed points were shifted normal to the cortex near the ROI border (dashed circle, distance from cortex = 5mm) *$p < 0.05$.
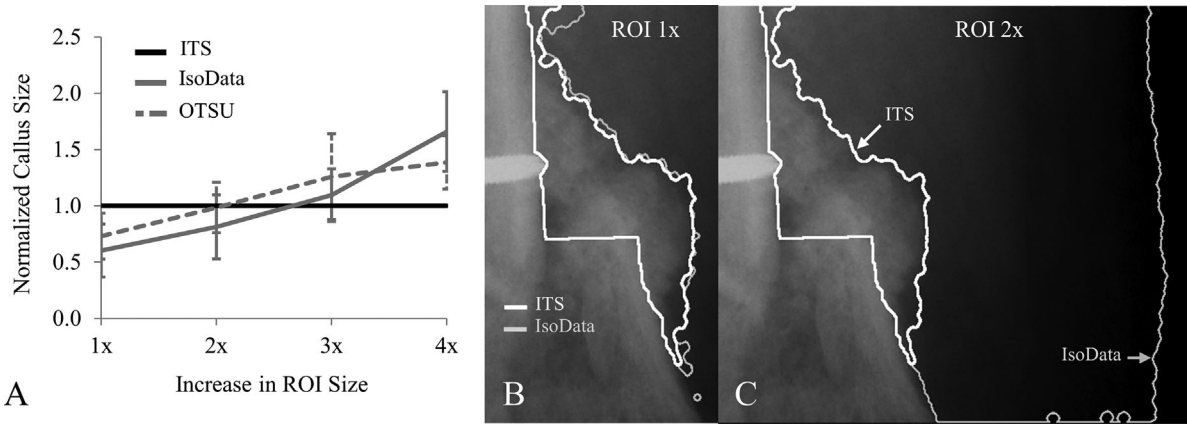
Figure 6. Effect of ROI size on callus segmentation. (A) The ITS method was the only method unaffected by changes to ROI area. (B) For example, the IsoData method might segment the callus similarly to the ITS for a specific ROI, (C) but changing the ROI area could affect the IsoData segmentation results, while the ITS results were unchanged.

measurement of callus size using the Otsu and Isodata algorithms was affected by ROI area (Fig. 6A; $p < 0.01$, $p < 0.01$, respectively). For this analysis, cortex segmentation was held constant as ROI area was increased to include a greater periosteal region (Fig. 6B and C).
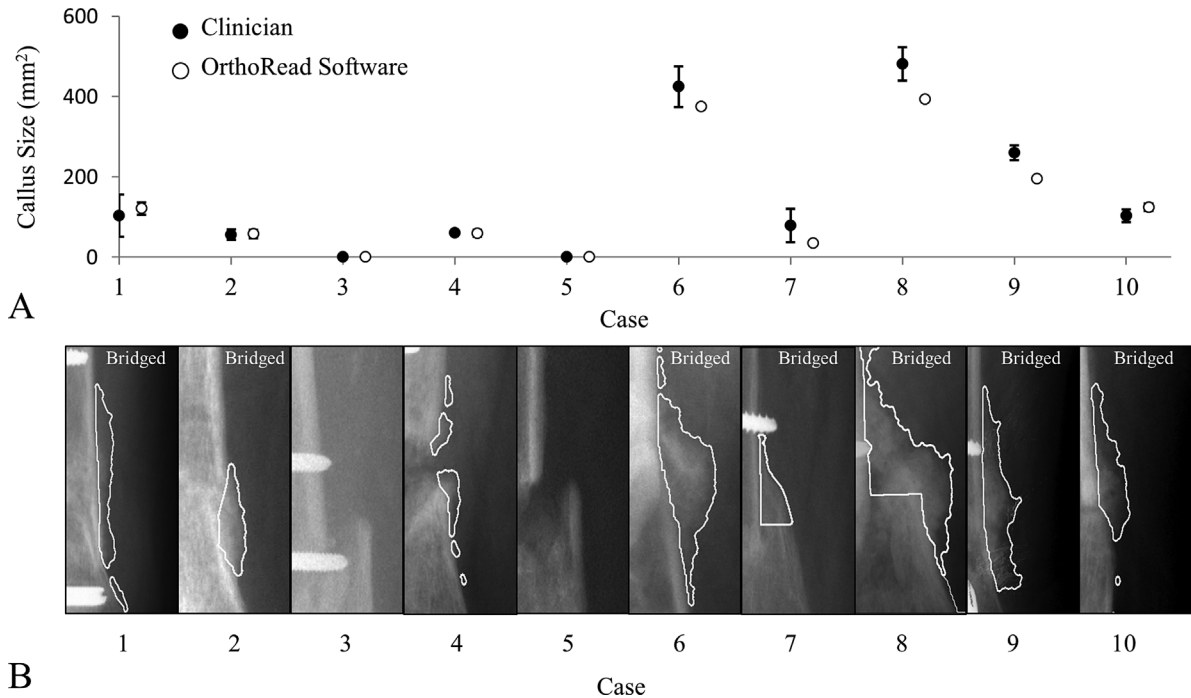
Clinical Validation

Overall, OrthoRead had a high positive correlation with the clinician group when outlining fracture callus (Fig. 7A, $R^2 = 0.98$, $p < 0.001$). For all ten cases, the average inter-observer variation in the OrthoRead group was 6% and in the clinician group was 22%. The runtime for OrthoRead to segment

cortex was $0.9 \pm 0.5\,s$, and to segment callus was $2.2 \pm 1.1\,s$ (200 PPI, 2.7 GHz processor). OrthoRead determined that seven of the ten cortices were bridged (Fig. 7B), which matched an independent analysis by orthopaedic surgeons.[20]

Experimental Validation

The callus specimens included in this analysis ranged in volume from 2,835 to 11,984 mm^3 (Fig. 8A) and in area from 148 to 961 mm^2 (Fig. 8B). The 2D area measurements acquired from plain radiographs and the 3D volume measurements acquired from μCT had a strong positive correlation (Fig. 8C; $R^2 = 0.70$, $p < 0.001$). Total analysis time to measure periosteal

Figure 7. Clinical validation of the image analysis software. (A) Results from OrthoRead had a high positive correlation to clinicians ($R^2 = 0.98$) and OrthoRead had 3× less inter-observer error. (B) Callus segmentation results for the ten cases using the ITS algorithm. The image analysis software also identified if the fracture gap was bridged.
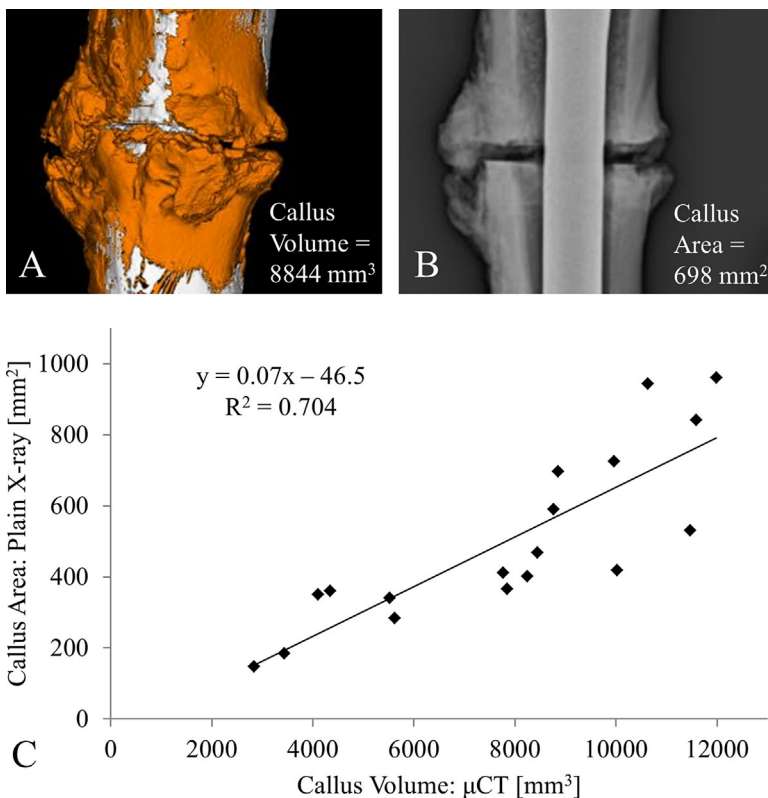
Figure 8. Comparison of 2D and 3D callus. Callus at ovine tibial fractures was measured using (A) µCT and (B) plain *x*-ray. (C) A strong positive correlation existed between 3D callus volume and 2D callus area.

callus area from all four cortices using OrthoRead was less than 10 min per case. Total analysis time to measure periosteal callus volume from µCT scans was 2.5–3 h per case.

DISCUSSION

This study has developed and validated robust algorithms to rapidly identify and quantify periosteal callus in digital radiographs. These algorithms were implemented into a software application, OrthoRead, which measured callus area with good accuracy and objectivity. The error of OrthoRead was less than 5% at different image resolutions, image rotations, and was insensitive to the size of the analyzed region of interest. The callus area detected by OrthoRead correlated extremely well with a previously published analysis by orthopaedic surgeons, and correlated well to the callus volume detected when using three-dimensional µCT. Moreover, the software improved the objectivity of callus measurement, as orthopaedic surgeons that manually outlined the callus had 22% inter-observer variability, while software operators with non-medical training had 6% inter-observer variability. OrthoRead has a run time of 3 s on a standard processor, and therefore, a user can open a digital radiograph and measure callus area in less than 1 min.

OrthoRead uses a novel ITS algorithm to segment the callus. This method is based on the flood filling of water shed lines to create callus objects, where the water shed lines are defined by the gradient image at iterative threshold levels. Threshold optimization is achieved based on two conditions: Stabilization of callus size between threshold iterations, and existence of a negative gradient along the majority of the border between the callus and background. An advantage of our ITS method is that threshold optimization is based on gradients and normalized parameters that act independently of the image resolution and the ROI size being analyzed. Whereas, Otsu and IsoData methods, which are popular image processing algorithms that also use threshold optimization, are based on an image's pixel intensity histogram. More specifically, the Otsu method maximizes the intra-class variance between the background and object (i.e., callus), and thus gives the best separation between two distinct classes of pixel intensity;[23] while the IsoData method uses an iterative technique to minimize the difference in the mean values of the background and object.[24] Changes to the ROI will alter the image's pixel intensity histogram, and therefore, will affect the between-class variance and mean values used by Otsu and IsoData, respectively. These mathematical differences in threshold optimization help explain why increasing the ROI by threefold resulted in an average increase in callus size of 40% when using the Otsu and IsoData methods, and only 0.01% when using our ITS method (Fig. 6). The segmentation algorithms used by OrthoRead are also invariant to rotation, and any measurable changes in callus area from rotation are due to intrinsic rounding errors from image rotation operations. This is an important improvement on a previous Matlab algorithm that required the long axis of the bone to be nearly vertical in

order to accurately detect callus.[18] Further, the previous Matlab algorithm used fixed global thresholding for callus segmentation, which is intrinsically less robust than the optimized global thresholding method used in the ITS algorithm. The development of the ITS algorithm was based on empirical observations and may be appropriate for other medical imaging applications, including the volumetric segmentation of callus using computed tomography.[27]

An innovation of OrthoRead is the novel implementation of an optimal boundary tracking method to expedite cortex segmentation. Optimal boundary tracking methods, such as intelligent scissors, are commonly used in commercial software to delineate objects of interest. These algorithms are semi-automated, and require the selection of seed points to instruct the segmentation of a contoured path along an edge.[21] Seed points are normally interactively defined at specified time intervals as the user manually moves a free point around the object of interest. In OrthoRead, the placement of seed points was modified so that the user manually clicks seed points on the cortex surface. There is no limit to the number of seed points the user can select, but the user must click two seed points per bone fragment. This study found that OrthoRead's accuracy in detecting callus was moderately insensitive to seed point placement. When cortex seed points were placed distal or proximal to the cortex surface, the error was less than 6%, even when the seed point was markedly misplaced (Fig. 4C). An advantage of this methodology is that it mitigates user error, while also minimizing user interaction. It also provides the necessary flexibility for users to apply cortex segmentation to a broad range of fracture morphologies. The simplicity of this method makes it intuitive and attractive for clinical applications.

This study showed that the projected callus area measured from plain radiographs has a strong positive correlation with callus volume measured from μCT. Previous investigators have shown that projected area from plain radiographs is well-correlated with area measured from a single image slice of a CT stack, but to our knowledge, this is the first study to directly compare the 2D periosteal callus area and full-3D periosteal callus volume from the same specimens. The strong positive correlation we found suggests that computerized image analysis of plain radiographs may be considered as an adjunct to or a replacement for CT scanning in preclinical and clinical investigations of fracture healing, especially when study cost and radiographic exposure are limiting factors. The measurement of 2D callus area may also be particularly useful for retrospective studies in which only plain films are available for a patient group, as plain radiographs are the standard imaging modality used for post-operative clinical visits.[5] We can further evaluate our correlation results by using the slope and y-intercept determined from linear regression of the experimental data (Fig. 8C) to predict 3D callus

volume from the 2D area measured by OrthoRead. Using this approach, we determined that the 2D projections would overestimate callus volume with an error of $7 \pm 25\%$ for all 16 cases. The high standard deviation in the volume prediction is likely due to the observed asymmetry of the callus formation around the fracture site; where depending on the fracture site location, the anteroposterior and lateral radiographs may capture a 2D projection of the callus volume with above average or below average callus size. Errors in prediction may also be caused by the enhanced resolution of μCT relative to plain radiography.

The development of OrthoRead advances computer vision in fracture care. To our knowledge, OrthoRead is the first public software that has been designed and validated to automate the measurement of periosteal callus in plain radiographs. Although previous algorithms have been developed to measure fracture callus,[16–18] they are not available as a public software application and have not undergone the rigorous validation applied in this study. OrthoRead is unique in that it has an intuitive graphic user interface (Fig. 2A) and uses fast and robust algorithms to optimize the segmentation of both the cortex and callus. OrthoRead is also a portable application, which allows users to run OrthoRead on all major operating systems without requiring installation (i.e., plug-and-play). Further, OrthoRead uses information from the cortex and callus segmentation results to report whether the callus has bridged the cortical fragments. Callus formation and cortical bridging are two of the three scoring criteria currently being used for qualitative radiographic assessment of fracture union in the tibia.[28] In the future, computer aided detection techniques could be incorporated into OrthoRead to automate the third scoring criteria, fracture line disappearance. This would further enhance the software's clinical utility and could lead to a quantitative gold standard for radiographic evaluation of fracture union.

This study has several limitations. Accuracy results are based on a surrogate model with a simplified callus structure, and should be interpreted accordingly. Although the callus segmentation algorithm used normalized parameters to identify an optimal threshold for each specific image, the algorithm also included morphological operations with fixed values that were applied to all images. These fixed values were optimized for images with 200 PPI, and accuracy may decrease at higher image resolutions. For example, during callus segmentation, a 3×3 circular structural element is used to smooth rough edges of the callus surface, and this smoothing operation will remove a lower percentage of callus area as PPI increases. This helps explain why OrthoRead predicted slightly greater callus area in the surrogate model for images with 300 PPI compared to 200 PPI. Accuracy is also dependent on proper unit conversion from pixels to metric area. This requires the user knowing the actual

dimension of a radiographic feature (e.g., screw diameter), and user's should be aware of differences that may exist between the actual measured size of an implant component and the nominal size quoted by the manufacturer. It is also important to note that while callus formation is an important indicator of healing in comminuted fractures treated with bridge plating or intramedullary nailing,[22,29] fracture healing can also occur without callus formation, as interfragmentary compression can promote healing without callus. Also, an inherent limitation of measuring callus in a two-dimensional radiograph is that it only approximates the three-dimensional structure of callus. However, in this study, we found that callus area calculated from plain radiographs correlated well with callus volume calculated from μCT.

Medical imaging technology may help reduce the incidence of delayed fracture healing and non-unions by providing an objective platform to evaluate competing treatment strategies. In this study, a software application named OrthoRead was developed and validated to measure fracture callus in plain radiographs. To our knowledge, OrthoRead is the first public software that has been designed and validated to automate the measurement of callus in plain radiographs. By being accurate, fast, and portable to multiple operating systems, OrthoRead can serve as an important scientific tool to quantify an outcome metric with clinical relevance. In a research setting, this software can support prospective and retrospective clinical studies investigating implant efficacy,[30] and can assist research on fracture healing mechanobiology.[31] In a clinical setting, this software could be used to quantitatively track healing progression and could support communication between clinicians and patients.

AUTHORS' CONTRIBUTION

Lead developer of software, testing and manuscript preparation (S.M.P.). Supervision and analysis of ovine x-rays and micro-CT images (H.L.D.). Reconstruction and measurement of 3D fracture callus from micro-CT (K.A.H.). Ovine surgeries, animal husbandry, x-rays, and postmortem analysis (K.K.). Ovine surgeries and clinical review of x-rays and micro-CT (J.A.H.). Experimental design, algorithm development, software design, and manuscript preparation (T.J.L.).

REFERENCES

1. Bhandari M, Guyatt G, Tornetta P, 3rd, et al. 2008. Randomized trial of reamed and unreamed intramedullary nailing of tibial shaft fractures. J Bone Joint Surg Am 90:2567–2578.
2. Schutz M, Muller M, Krettek C, et al. 2001. Minimally invasive fracture stabilization of distal femoral fractures with the LISS: a prospective multicenter study. Results of a clinical study with special emphasis on difficult cases. Injury 32:SC48–SC54.
3. Fankhauser F, Gruber G, Schippinger G, et al. 2004. Minimal-invasive treatment of distal femoral fractures with the LISS (less invasive stabilization system): a prospective study of 30 fractures with a follow up of 20 months. Acta Orthop Scand 75:56–60.
4. Antonova E, Le TK, Burge R, et al. 2013. Tibia shaft fractures: costly burden of nonunions. BMC Musculoskelet Disord 14:42.
5. Ghattas TN, Dart BR, Pollock AG, et al. 2013. Effect of initial postoperative visit radiographs on treatment plans. J Bone Joint Surg Am 95:e571–e574, S571.
6. Hammer RR, Hammerby S, Lindholm B. 1985. Accuracy of radiologic assessment of tibial shaft fracture union in humans. Clin Orthop Relat Res 199:233–238.
7. Tower SS, Beals RK, Duwelius PJ. 1993. Resonant frequency analysis of the tibia as a measure of fracture healing. J Orthop Trauma 7:552–557.
8. Panjabi MM, Walter SD, Karuda M, et al. 1985. Correlations of radiographic analysis of healing fractures with strength: a statistical analysis of experimental osteotomies. J Orthop Res 3:212–218.
9. Corrales LA, Morshed S, Bhandari M, et al. 2008. Variability in the assessment of fracture-healing in orthopaedic trauma studies. J Bone Joint Surg Am 90:1862–1868.
10. Bhandari M, Guyatt GH, Swiontkowski MF, et al. 2002. A lack of consensus in the assessment of fracture healing among orthopaedic surgeons. J Orthop Trauma 16:562–566.
11. Whelan DB, Bhandari M, McKee MD, et al. 2002. Interobserver and intraobserver variation in the assessment of the healing of tibial fractures after intramedullary fixation. J Bone Joint Surg Br 84:15–18.
12. Tiedeman JJ, Lippiello L, Connolly JF, et al. 1990. Quantitative roentgenographic densitometry for assessing fracture healing. Clin Orthop Relat Res 253:279–286.
13. Eastaugh-Waring SJ, Joslin CC, Hardy JR, et al. 2009. Quantification of fracture healing from radiographs using the maximum callus index. Clin Orthop Relat Res 467:1986–1991.
14. Whelan DB, Bhandari M, Stephen D, et al. 2010. Development of the radiographic union score for tibial fractures for the assessment of tibial fracture healing after intramedullary fixation. J Trauma 68:629–632.
15. Bhandari M, Chiavaras MM, Parasu N, et al. 2013. Radiographic union score for hip substantially improves agreement between surgeons and radiologists. BMC Musculoskelet Disord 14:70.
16. Augat P, Merk J, Genant HK, et al. 1997. Quantitative assessment of experimental fracture repair by peripheral computed tomography. Calcif Tissue Int 60:194–199.
17. Morcuende JA, Gomez P, Stack J, et al. 2004. Effect of chemotherapy on segmental bone healing enhanced by rhBMP-2. Iowa Orthop J 24:36–42.
18. Lujan TJ, Madey SM, Fitzpatrick DC, et al. 2010. A computational technique to measure fracture callus in radiographs. J Biomech 43:792–795.
19. Lujan TJ, Henderson CE, Madey SM, et al. 2010. Locked plating of distal femur fractures leads to inconsistent and asymmetric callus formation. J Orthop Trauma 24:156–162.
20. Henderson CE, Lujan TJ, Kuhl LL, et al. 2011. 2010 mid-America orthopaedic association physician in training award: healing complications are common after locked plating for distal femur fractures. Clin Orthop Relat Res 469:1757–1765.
21. Liang J, McInerney T, Terzopoulos D. 2006. United snakes. Med Image Anal 10:215–233.
22. Marsh D. 1998. Concepts of fracture union, delayed union, and nonunion. Clin Orthop Relat Res 355:S22–S30.
23. Otsu N. 1979. A threshold selection method from gray-level histograms. IEEE Trans Syst Man Cybern 9:62–66.
24. Memarsadeghi N, Mount DM, Netanyahou NS, et al. 2007. A fast implementation of the isodata clustering algorithm. Int J Comput Geometry Appl 71–103.
25. Ding M, Odgaard A, Hvid I. 1999. Accuracy of cancellous bone volume fraction measured by micro-CT scanning. J Biomech 32:323–326.

26. Freeman TA, Patel P, Parvizi J, et al. 2009. Micro-CT analysis with multiple thresholds allows detection of bone formation and resorption during ultrasound-treated fracture healing. J Orthop Res 27:673–679.
27. Augat P, Merk J, Ignatius A, et al. 1996. Early, full weightbearing with flexible fixation delays fracture healing. Clin Orthop Relat Res 328:194–202.
28. Kooistra BW, Dijkman BG, Busse JW, et al. 2010. The radiographic union scale in tibial fractures: reliability and validity. J Orthop Trauma 24:S81–S86.
29. Ruedi TP, Buckley RE, Moran CG. 2007. AO Principles of fracture management. New York, NY: Thieme.
30. Henderson CE, Lujan T, Bottlang M, et al. 2010. Stabilization of distal femur fractures with intramedullary nails and locking plates: differences in callus formation. Iowa Orthop J 30:61–68.
31. Augat P, Simon U, Liedert A, et al. 2005. Mechanics and mechano-biology of fracture healing in normal and osteoporotic bone. Osteoporos Int 16:S36–S43.